SPANDIDOS PUBLICATIONS

ONCOLOGY LETTERS 20: 43-52, 2020

YRDC is upregulated in non-small cell lung cancer and promotes cell proliferation by decreasing cell apoptosis

HAIBO SHEN*, ENKUO ZHENG*, ZHENHUA YANG, MINGLEI YANG, XIANG XU, YINJIE ZHOU, JUNJUN NI, RUI LI and GUOFANG ZHAO

Cardiothoracic Surgery Department, Hwa Mei Hospital, University of Chinese Academy of Sciences, Ningbo, Zhejiang 315010, P.R. China

Received January 6, 2019; Accepted September 20, 2019

DOI: 10.3892/ol.2020.11560

Abstract. Non-small cell lung cancer (NSCLC) is the leading cause of cancer-associated mortality worldwide. yrdC N6-threonylcarbamoltransferase domain containing protein (YRDC) has been demonstrated to be involved in the formation of threonylcarbamoyladenosine in transfer ribonucleic acid. However, the molecular mechanisms underlying NSCLC progression remain largely unclear. The present study revealed that YRDC was upregulated in NSCLC samples compared with adjacent non-cancerous tissues by analyzing datasets obtained from the Gene Expression Omnibus and The Cancer Genome Atlas. Higher expression of YRDC was associated with overall survival time and disease-free survival time in patients with NSCLC, particularly in lung adenocarcinoma. Furthermore, knockdown of YRDC in NSCLS cell lines significantly suppressed cell growth and cell colony formation *in vitro*. Additionally, the results demonstrated that silencing of YRDC induced apoptosis of A549 cells. Then, the protein-protein interaction networks associated with yrdC N6-threonylcarbamoltransferase domain containing protein (YRDC) in NSCLC were subsequently constructed to investigate the potential molecular mechanism underlying the role of YRDC in NSCLC. The results revealed that YRDC was involved in the regulation of spliceosomes, ribosomes, the p53 signaling pathway, proteasomes, the cell cycle and DNA replication. The present study demonstrated that YRDC may serve as a novel biomarker for the prognosis prediction and treatment of NSCLC.

Correspondence to: Professor Guofang Zhao, Cardiothoracic Surgery Department, Hwa Mei Hospital, University of Chinese Academy of Sciences, 41 Northwest Street, Ningbo, Zhejiang 315010, P.R. China
E-mail: nbzhaoguofang@hotmail.com

*Contributed equally

Key words: non-small cell lung cancer, yrdC N6-threonylcarbamoltransferase domain containing protein, biomarker, proliferation, apoptosis

Introduction

Non-small cell lung carcinoma (NSCLC) accounts for >80% of patients with lung cancer, and was a leading cause of cancer-associated mortality, both worldwide and in China (2008) (1,2). Over the past decade, increasing efforts have been made to identify novel biomarkers and classify the molecular mechanisms underlying NSCLC progression (3-5). However, an urgent need to identify novel drivers and biomarkers for NSCLC remains.

Currently, >150 RNA post-transcriptional modifications had been identified, including N6-methyladenosine (m6A) (6), threonylcarbamoyladenosine (t6A) (7) and pseudouridine (8,9) modifications of ribosomal RNA and transfer RNA (tRNA). Emerging studies have demonstrated that RNA modifications serve crucial roles in human cells (10-12). For example, m6A modifications of mRNAs influenced RNA stability and translation (11) and t6A modification at position 37 of adenosine-starting codons decoding tRNAs imparted a unique structure to the anticodon loop, which enhanced its binding to ribosomes *in vitro* (7,12). yrdC N6-threonylcarbamoltransferase domain containing protein (YRDC) has been revealed to be involved in the formation of t6A in tRNA (13). Previous studies have indicated that dysregulation of YRDC expression was associated with the progression of bladder cancer; YRDC expression was upregulated in bladder cancer samples and knockdown of YRDC significantly suppressed bladder cancer cell proliferation (14). However, the molecular mechanisms underlying YRDC in NSCLC remain unclear.

The present study aimed to elucidate the prognostic value and functional roles of YRDC in NSCLC, and to assess the expression levels of YRDC in NSCLC samples compared with normal samples. The association between YRDC expression and survival time was evaluated using the Kaplan-Meier Plotter database. The present study also knocked-down YRDC in NSCLC cells in order to evaluate the influence of YRDC on proliferation and apoptosis. These analyses will provide evidence to support the concept that YRDC could act as a biomarker for the prognosis prediction and treatment of NSCLC.

Materials and methods

Cell culture. The NSCLC cell lines A549, H1975 and H1299 were purchased from the Cell Bank of Type Culture Collection

of Chinese Academy of Sciences and cultured in RPMI-1640 medium (HyClone; GE Healthcare Life Sciences) supplemented with 10% bovine serum, penicillin (100 U/ml) and streptomycin (100 U/ml; all Gibco; Thermo Fisher Scientific, Inc.). A549 cells were incubated at 37˚C in a humidified atmosphere consisting of 95% air and 5% CO_2.

Construction of YRDC knockdown lentivirus. The short hairpin (sh)RNA sequence targeting YRDC (5'-CCGGCAGTTCTCTGAATGTCGAGGACTCGAGTCCTCGACATTCAGAGAACTGTTTTT-3') was obtained from Shanghai Genechem Co., Ltd. Recombinant lentiviral vectors were constructed as previously described (15). The empty GV115 lentiviral vector (Shanghai Genechem Co., Ltd.) was used as the short hairpin (sh)RNA control. A total of 6 μg SureSilencing shRNA plasmids (Qiagen GmbH) and shRNA control were transfected to knockdown YRDC expression levels, using standard molecular techniques. At 48 h post-transfection, the transfection efficiency of shYRDC was determined using reverse transcription-quantitative (RT-q)PCR and western blotting.

Western blot analysis. The western blot analysis was performed as previously described (16). The antibodies used in the present study included anti-YRDC (1:1,000; cat. no. ab70795; Abcam) and anti-GAPDH (1:1,000; cat. no. sc-32233; Santa Cruz Biotechnology, Inc.). Secondary antibodies (Goat anti-mouse and goat anti-rabbit IgG-horseradish peroxidase; 1:5,000; cat. no. A9044 and cat. no. A9169, respectively; Sigma-Aldrich; Merck KGaA) were purchased from Sigma-Aldrich; Merck KGaA.

RT-qPCR. RT-qPCR was performed as previously described (17). Total RNA was extracted from A549, H1975 and H1299 cells using TRIzol® reagent (Invitrogen; Thermo Fisher Scientific, Inc.), and cDNA was synthesized using a RevertAid First Strand cDNA Synthesis kit (Promega Corporation) according to the manufacturers' protocol. miScriptSYBR GreenPCR kit (Qiagen, Inc.) was used to perform the qPCR. The qPCR primers used in the present study were: YRDC forward, 5'-GGCGTCCAAGACCCACATC-3' and reverse, 5'-ACAGGCCACTTTAAGCATTCC-3'; and GAPDH forward, 5'-TGACTTCAACAGCGACACCCA-3' and reverse, 5'-CACCCTGTTGCTGTAGCCAAA-3'. The $2^{-\Delta\Delta Cq}$ method was used to calculate the relative expression levels of the target genes (18).

Cell proliferation and viability assays. The adherent cell cytometry system, Celigo® (Celigo Inc.), was used to detect the cell proliferation in A549 cells, as previously described (15). Plates were analyzed using an adherent cell cytometer equipped with bright field and fluorescent channels. Gating parameters were adjusted for each fluorescence channel to exclude background and other non-specific signals. The Celigo® system provided a gross quantitative analysis for each fluorescence channel and individual well, including total count and average integrated red fluorescence intensity of gated events. Fluorescence images were detected using a fluorescence microscope at x200 magnification. An MTT assay was performed as previously described (19). A total of $2x10^3$ A549 cells were seeded and cultured in 96-well plates for 5 days at 37˚C in 5% CO_2. Cells were stained with MTT dye (0.5 mg/ml; Sigma Aldrich; Merck KGaA) for 2 h at 37˚C. The cell culture medium was removed and replaced with 150 ml dimethyl sulfoxide (Sigma Aldrich; Merck KGaA) to dissolve the purple formazan crystals. The absorbance was subsequently measured at a wavelength of 570 nm, with 655 nm as the reference wavelength.

Cell apoptosis assay. For the cell apoptosis assay, A549 cells ($3x10^5$/well) were seeded into 6-well plates and assayed with an Annexin V-APC Apoptosis Detection kit (eBioscience; Thermo Fisher Scientific, Inc.) 48 h after transfection according to the manufacturer's protocol. Apoptotic cells were subsequently detected using a flow cytometer (FACScalibur; Becton, Dickinson and Company). The results were obtained by analyzing the data with FlowJo software (version 7.6.1; FlowJo, LLC, Ashland, OR, USA).

Colony formation assays. A549 cells were plated into 6-well plates at a density of 500 cells/well. After 10 days, the colonies were stained with 1% crystal violet (Sigma-Aldrich; Merck KGaA) for 30 sec at room temperature following fixation with 4% paraformaldehyde for 5 min at room temperature. Images of the cell colonies were captured using an inverted light microscope (magnification, x200; MicroPublisher 3.3RTV; Olympus Corporation).

Public datasets analysis. The Cancer Genome Atlas (TCGA) Lung Cancer Cohort data, (http://tcga.cancer.gov/dataportal; accessed June 2016), which includes the lung adenocarcinoma (LUAD) cohort (comprising 517 primary LUAD tissues and 59 adjacent non-cancerous tissues) and the lung squamous cell carcinoma (LUSC) cohort (comprising 501 primary LUSC tissues and 51 adjacent non-cancerous tissues) were downloaded from the Firebrowse database (http://firebrowse.org/). The YRDC expression levels were also compared between NSCLC and adjacent non-cancerous tissues using public datasets including GSE18842 (20), GSE19804 (21) and GSE19188 (22). Moreover, the present study then analyzed a public dataset Depmap (https://depmap.org/portal/gene/YRDC?tab=dependency) to further validate the roles of YRDC. The gene-level differential dependency scores are available on at https://depmap.org/rnai/index.

Kaplan-Meier Plotter analysis. Kaplan-Meier curves were created using the Kaplan-Meier Plotter (www.kmplot.com) (17) in order to analyze the prognostic value of YRDC expression. The Kaplan-Meier Plotter is capable of assessing the effect of 54,675 genes on survival time using 10,293 cancer samples, including 5,143 breast cancer, 1,648 ovarian cancer, 2,437 lung cancer and 1,065 gastric cancer samples, with mean follow-up periods of 69, 40, 49 and 33 months, respectively. Patients with NSCLC were divided into high- and low-expression groups based on the median expression level of YRDC (Cutoff value for OS analysis, 717; Cutoff value for DFS analysis, 796) in order to evaluate the overall survival (OS) time and disease-free survival (DFS) time. The OS and DFS rate estimates were calculated using the Kaplan-Meier method with the log-rank test.

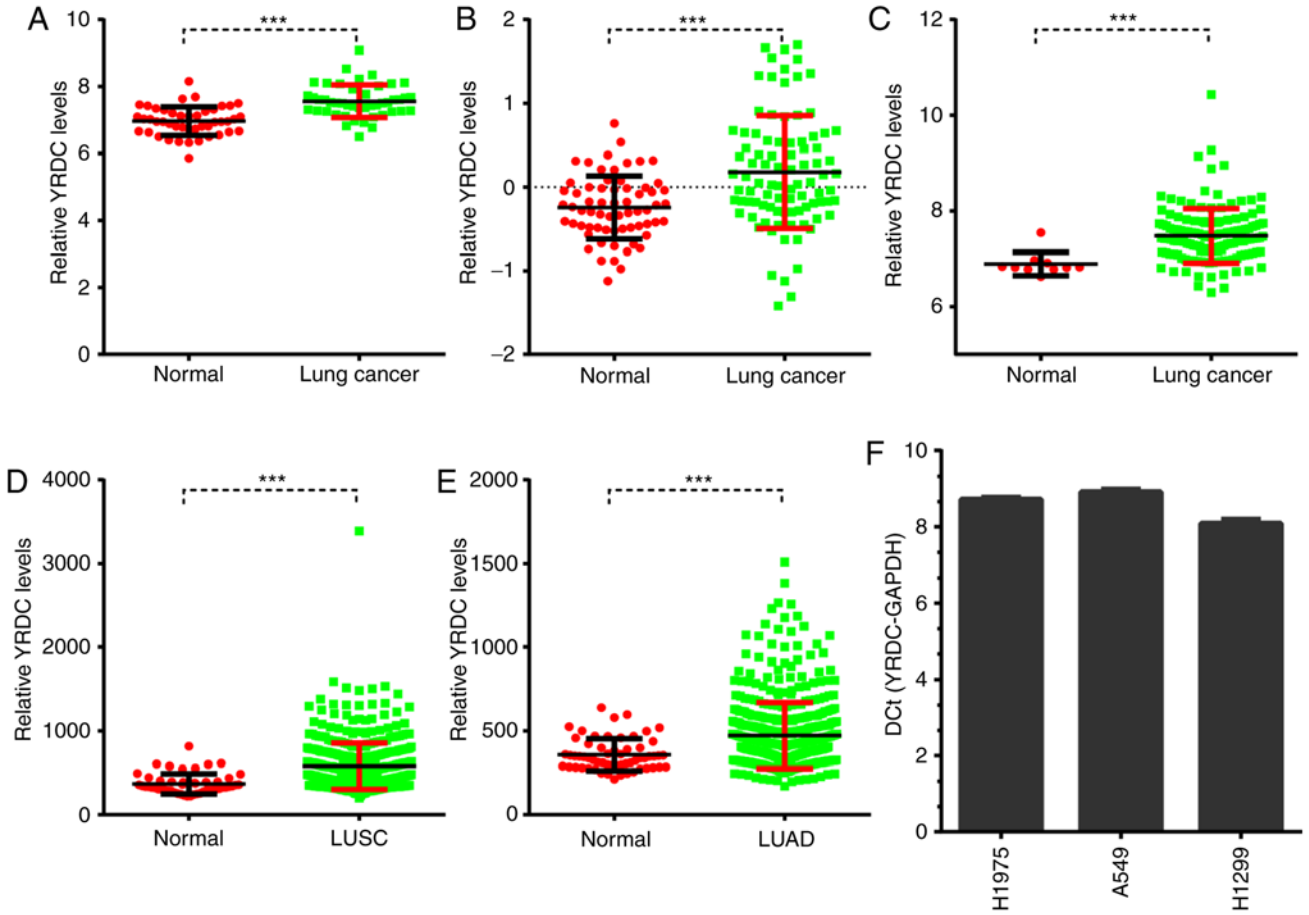

Figure 1. YRDC was upregulated in NSCLC. YRDC expression levels in NSCLC samples were compared with normal samples by analyzing the (A) GSE30219, (B) GSE19188 and (C) GSE18842 datasets. YRDC was upregulated in NSCLC samples compared with normal samples by analyzing (D) LUAD and (E) LUSC. (F) The expression of YRDC in 3 NSCLC cell lines, including H1975, A549 and H1299 cells, compared with the expression of GAPDH. ***P<0.001 vs. adjacent non-cancerous tissues. YRDC, yrdC N6-threonylcarbamoyltransferase domain containing protein; NSCLC, non-small cell lung carcinoma; LUAD, lung adenocarcinoma; LUSC, lung squamous cell carcinoma; HR, hazard ratio.

Protein-protein interaction (PPI) network and module analysis. Correlations between the expression of YRDC and target gene expression in lung cancer were analyzed using the cBioPortal database (http://www.cbioportal.org/index.do). The top 1,000 co-expressing mRNAs were considered as potential downstream targets of YRDC in NSCLC. The present study constructed a PPI network using The Search Tool for the Retrieval of Interacting Genes (STRING; version 10.5; https://string-db.org) (23). YRDC-mediated PPI networks were constructed in NSCLC datasets using the STRING database (The threshold was a combined score of >0.4). The PPI network was presented using Cytoscape software (version 3.6.0; http://www.cytoscape.org) (24). The Mcode plugin (version 1.5.1; Bader Lab; University of Toronto) (25) was then used to identify key modules (degree cut-off ≥2 and the nodes with edges ≥2-core) in this network. The ClueGO plug-in in Cytoscape software (version 2.5.0; http://www.cytoscape.org/) was used to identify genes associated with Gene Ontology (http://geneontology.org/) terms (26). P<0.05 indicated a statistically significant difference.

Statistical analysis. SPSS v. 19.0 (IBM Corp.) was used for all statistical analyses. Results are expressed as the mean ± standard deviation. The unpaired Student's t-test was used to calculate statistical significance of YRDC expression levels between normal tissues and NSCLC samples. For more than two groups, one-way analysis of variance followed by the Newman-Keuls post-hoc test was used. Each experiment was performed in triplicate. P<0.05 was considered to indicate a statistically significant difference.

Results

YRDC is upregulated in NSCLC samples. The present study compared the YRDC expression levels between NSCLC and adjacent non-cancerous tissues using public datasets. A total of three GEO datasets were screened in order to investigate the expression pattern of YRDC in NSCLC. It was observed that YRDC was significantly upregulated in NSCLC compared with normal samples in GSE18842 (P<0.001), GSE19804 (P<0.001) and GSE19188 (P<0.001; Fig. 1A-C).

Furthermore, The Cancer Genome Atlas (TCGA) datasets were analyzed to validate the aforementioned GEO dataset analyses. TCGA lung adenocarcincoma (LUAD) dataset included 59 normal and 517 LUAD samples, and TCGA lung squamous cell carcinoma (LUSC) dataset included 51 normal and 501 LUSC samples. As presented in Fig. 1, the present

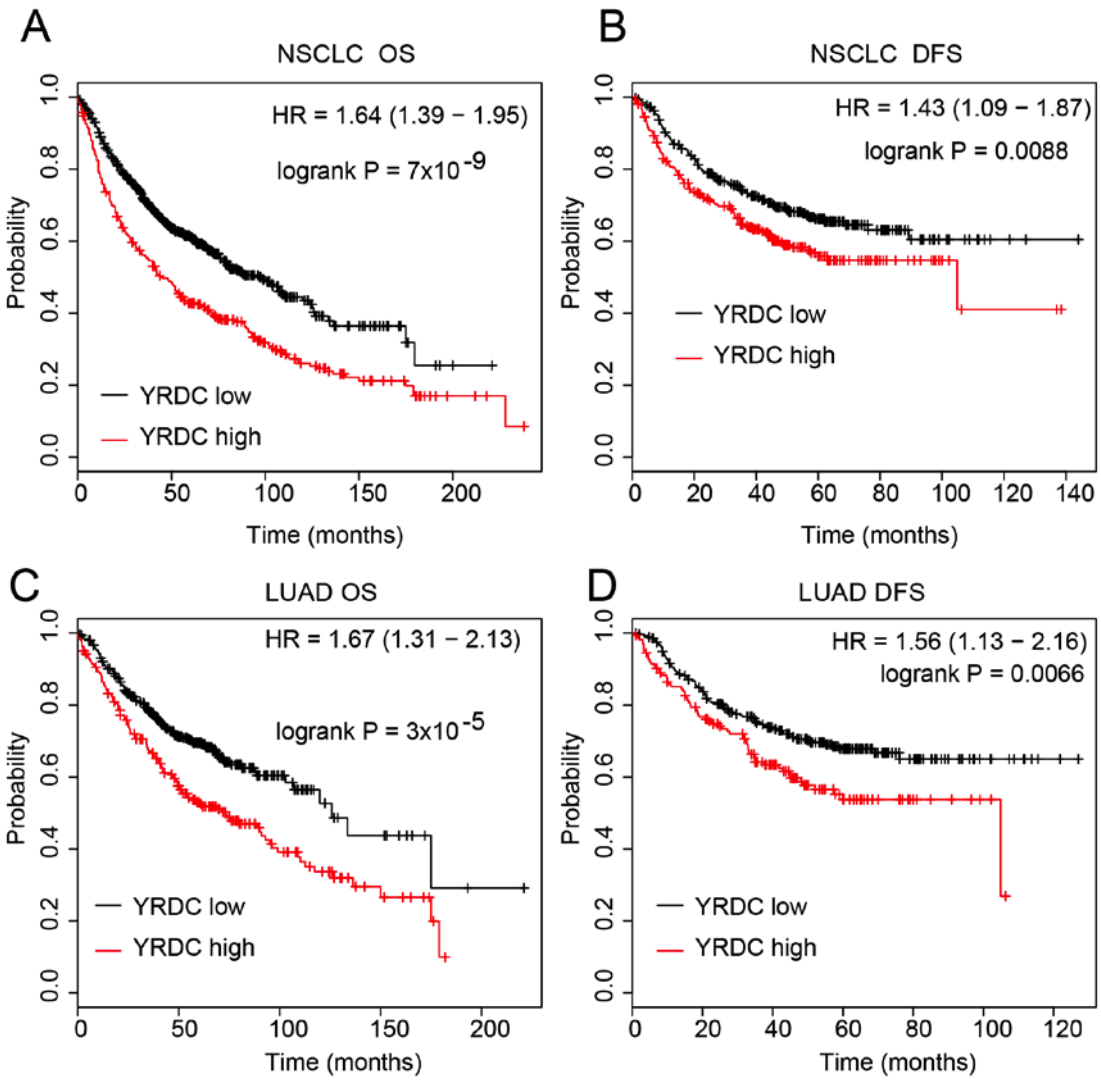

Figure 2. Higher YRDC expression was associated with shorter overall survival and disease-free survival time in NSCLC. Higher YRDC expression was associated with (A) shorter overall survival time and (B) disease-free survival time in NSCLC using Kaplan-Meier Plotter. Higher YRDC expression was associated with (C) shorter overall survival time and (D) disease-free survival time in lung adenocarcinoma using Kaplan-Meier Plotter. YRDC, yrdC N6-threonylcarbamoyltransferase domain containing protein; NSCLC, non-small cell lung carcinoma; HR, hazard ratio.

study demonstrated that YRDC was upregulated in both LUAD (P<0.05) and LUSC (P<0.05) samples compared with normal tissues (Fig. 1D and E). Of note, the absolute expression of YRDC in 3 NSCLC cell lines (H1975, A549 and H1299 cells) was compared with the expression of GAPDH. It was observed that YRDC was expressed in these NSCLC cell lines (Fig. 1F).

YRDC is associated with poor prognosis in patients with NSCLC. The present study performed a Kaplan Meier curve analysis of YRDC using the Kaplan Meier plotter database in order to further investigate the clinical importance of YRDC in NSCLC. The results revealed that compared with low expression, high expression of YRDC was associated with shorter OS (P<0.0001) and DFS time (P<0.01) in lung cancer (Fig. 2A and B). The association between YRDC expression and survival time in LUAD and LUSC was then assessed. This further analysis revealed that higher expression of YRDC was significantly associated with shorter OS (P<0.0001) and DFS (P<0.01) time in LUAD (Fig. 2C and D). These results suggested that YRDC may serve as a biomarker for the prognosis prediction of LUAD.

Bioinformatics analysis reveals the potential molecular mechanisms underlying YRDC in the progression of NSCLC. The molecular mechanism underlying YRDC in NSCLC previously remained largely unclear. In the present study, a co-expression analysis of YRDC in NSCLC was performed using a dataset downloaded from TCGA. The top 1,000 co-expressing mRNAs were considered as the potential downstream targets of YRDC in NSCLC.

Furthermore, the present study constructed YRDC-mediated PPI networks in NSCLC using the STRING database (combined score >0.4). The Mcode plugin was used to identify key modules (degree cut-off ≥2 and the nodes with edges ≥2-core) in this network. The top three hub modules are presented in Fig. 3. Module 1 contained 79 nodes and 2,145 edges, module 2 contained 38 nodes and 987 edges and module 3 contained 52 nodes and 845 edges (Fig. 3A-C).

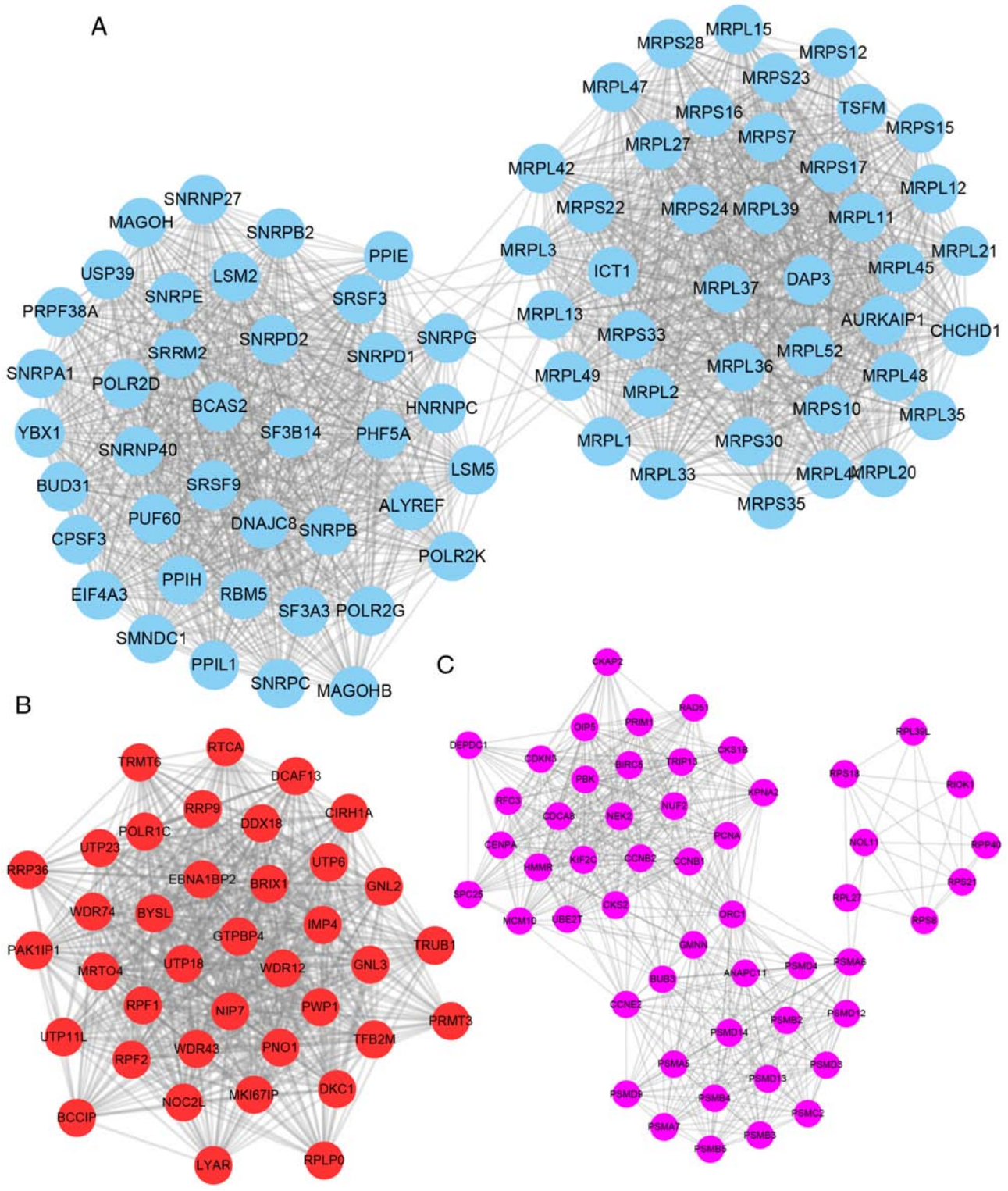

Figure 3. Construction of key YRDC mediated protein-protein interaction networks. (A) Module 1 contained 79 nodes and 2,145 edges, (B) module 2 contained 38 nodes and 987 edges and (C) module 3 contained 52 nodes and 845 edges. Blue nodes indicate nodes in Module 1. Red nodes indicate nodes in Module 2. Purple nodes indicate nodes in Module 3. YRDC, yrdC N6-threonylcarbamoyltransferase domain containing protein.

Functional annotation of YRDC-mediated hub PPI networks in NSCLC. The present study next performed a bioinformatics analysis of YRDC-mediated hub PPI networks in NSCLC using the ClueGo plug-in in Cytoscape. The results revealed that YRDC-associated module 1 was involved in regulating spliceosomes, the mRNA surveillance pathway, ribosomes and RNA polymerase (Fig. 4A); module 2 was involved in regulating ribosome biogenesis in eukaryotes (Fig. 4B); and module 3 was involved in the regulation of the p53 signaling pathway, proteasomes, the cell cycle and DNA replication (Fig. 4C).

Silencing of YRDC inhibits A549 cell proliferation and cell colony formation. The aforementioned bioinformatics analysis

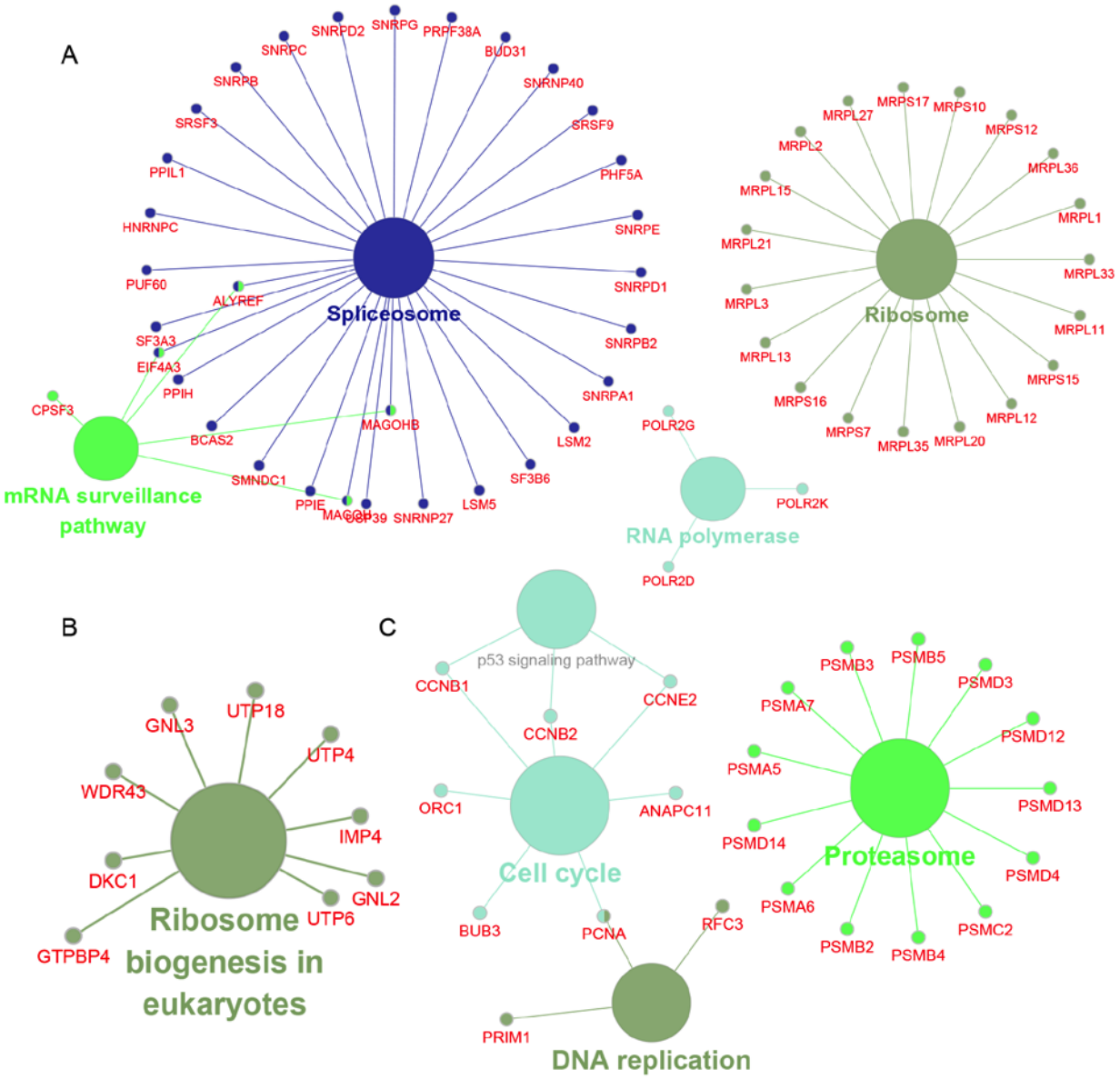

Figure 4. Bioinformatics analysis of YRDC-mediated hub protein-protein interaction networks in NSCLC. (A) YRDC-associated module 1 was involved in regulating spliceosomes, the mRNA surveillance pathway, ribosomes and RNA polymerase. (B) Module 2 was involved in regulating ribosome biogenesis in eukaryotes. (C) Module 3 was involved in the regulation of the p53 signaling pathway, proteasomes, the cell cycle and DNA replication. YRDC, yrdC N6-threonylcarbamoyltransferase domain containing protein; NSCLC, non-small cell lung carcinoma.

revealed that YRDC was involved in regulating cell proliferation-associated biological processes, such as p53 signaling, the cell cycle and DNA replication. In order to validate these findings, the present study performed loss-of-function assays using A549 cells. The present study successfully knocked-down the mRNA and protein expression levels of YRDC in A549 cells using a shRNA against YRDC (Fig. 5A and B).

The present study then performed two different types of assay in order to assess the influence of YRDC on tumor growth. Celigo® cell counting assay revealed that silencing of YRDC markedly suppressed A549 cell proliferation. The relative cell number in YRDC knockdown group decreased by >80% in comparison with the control group (P<0.001, Fig. 5C-E) 5 days after transfection. A similar effect on cell viability was also observed using the MTT assay (P<0.001, Fig. 5F-G). YRDC knockdown could inhibit cell growth by >80% compared with the control. The present study then analyzed a public dataset Depmap (https://depmap.org/portal/gene/YRDC?tab=dependency) to further validate the roles of YRDC. The present results demonstrated that knockdown of YRDC significantly suppressed the growth of several NSCLC cell lines (Fig. S1).

Furthermore, the cell colony formation assay was conducted in order to determine the roles of YRDC in regulating NSCLC growth. YRDC knockdown markedly inhibited the ability of A549 cells to form colonies compared with controls. The cell colonies in the YRDC knockdown group decreased by 75% compared with the control group (P<0.001, Fig. 6A and B). The current results suggest that YRDC may serve as an oncogenic factor in NSCLC.

Knockdown of YRDC induces cell apoptosis in NSCLC cells. Dysregulation of the apoptotic pathways is considered to be a hallmark of human cancer (27). The present study performed

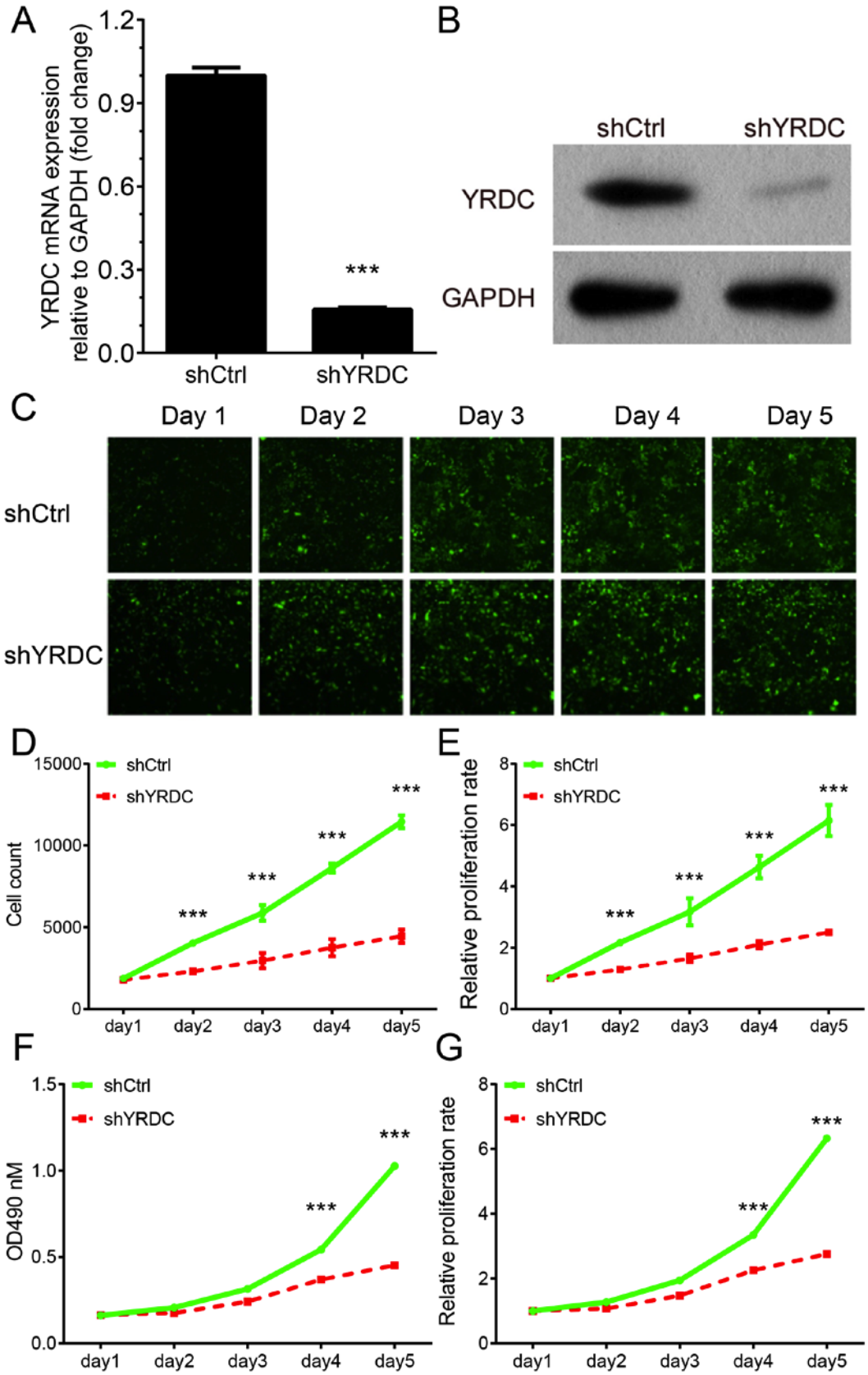

Figure 5. Knockdown of YRDC suppressed NSCLC proliferation and viability. The mRNA and protein levels of YRDC were detected following transfection with specific shRNA using (A) reverse transcription-quantitative PCR and (B) western blot analysis. (C) Celigo® cell counting assay showed the fluorescence images of A549 cells infected with shYRDC or shCtrl lentivirus (x200 magnification). Fluorescence images was detected by a fluorescence microscope at x200 magnification. (D) Cell counts of A549 cells infected with shYRDC lentivirus and shCtrl lentivirus using Celigo® cell counting assay. (E) Proliferation rates of A549 cells infected with shYRDC lentivirus and shCtrl lentivirus using Celigo® cell counting assay. (F) OD490 of A549 cells infected with shYRDC lentivirus and shCtrl lentivirus using MTT assay. (G) Proliferation rates of A549 cells infected with shYRDC lentivirus and shCtrl lentivirus using MTT assay. Data are presented as the mean ± standard deviation; n=3. ***P<0.001 compared to negative control group. YRDC, yrdC N6-Threonylcarbamoyltransferase Domain Containing protein; NSCLC, non-small cell lung carcinoma; shRNA, short hairpin RNA; OD, optical density.

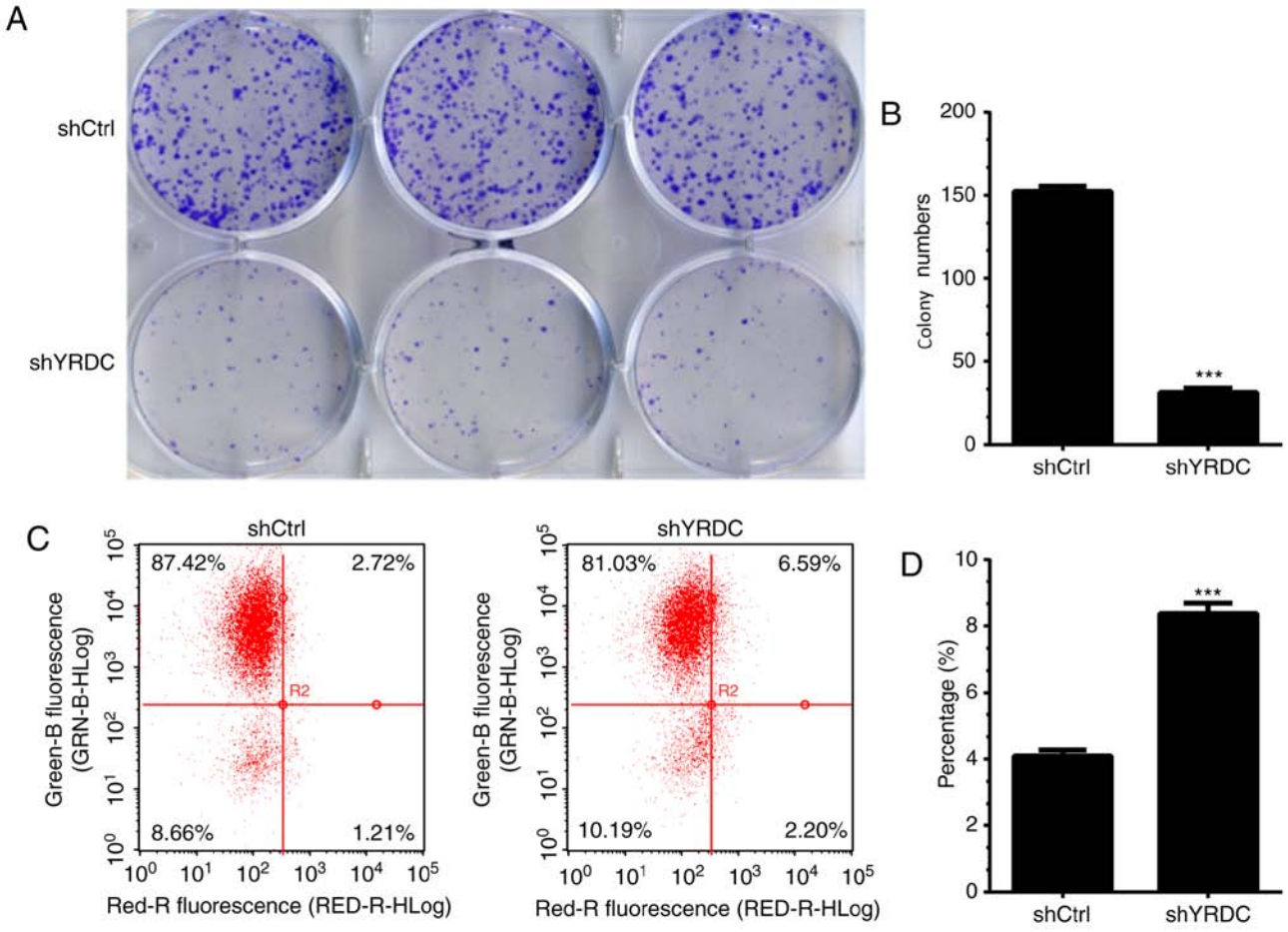

Figure 6. Knockdown of YRDC suppressed NSCLC cell colony formation and induced apoptosis. (A) Representative images showing cell colony formation results in A549 cells. (B) Statistical analysis showed that YRDC knockdown significantly inhibited NSCLC cell colony formation. (C) Representative images showing apoptosis results in A549 cells. (D) Statistical analysis showed that YRDC knockdown significantly induced NSCLC cell apoptosis. Data are presented as the mean ± standard deviation; n=3. ***P<0.001 compared with the negative control group. YRDC, yrdC N6-threonylcarbamoyltransferase domain containing protein; NSCLC, non-small cell lung carcinoma; shRNA, short hairpin RNA.

an annexin V-APC staining assay in order to determine the influence of YRDC on cell apoptosis in NSCLC. The percentage of apoptotic A549 cells significantly increased by 50% in the YRDC knockdown group when compared with the control group (P<0.001, Fig. 6C and D) 5 days after transfection, suggesting that YRDC plays an oncogenic role in NSCLC, at least in part, by suppressing cell apoptosis.

Discussion

Lung cancer is one of most common types of human cancer in China (28). In the past decade, an increasing amount of research has focused on the identification of novel biomarkers and drivers of cancer in NSCLC (29-31). A series of regulators associated with NSCLC proliferation and metastasis have been identified. For example, polycomb repressive complex 2 played crucial roles in Kirsten rat sarcoma virus-driven NSCLC progression (30), NOVA alternative splicing regulator 1 promoted NSCLC cell growth by regulating RNA splicing of human telomerase reverse transcriptase, and YEATS domain containing 2 regulated NSCLC tumorigenesis by regulating histone acetylation (31). However, the molecular mechanisms underlying NSCLC remained unclear. In the present study, it was revealed that YRDC served as an oncogene in NSCLC. Knockdown of YRDC in the NSCLC cell line A549 suppressed proliferation and cell colony formation, but induced A549 cell apoptosis.

The functions of YRDC in human cancer remains largely unclear. Previous studies have indicated that YRDC may serve as a subunit for a tRNA threonylcarbamoyl transferase, and was involved in the formation of t6A modification in tRNA (13,32). The aberrant protein translation was revealed to be associated with the progression of human cancer, such as glioma (33,34). A recent study reported that YRDC was upregulated in tumor samples compared with adjacent non-cancerous tissues, and promoted cancer cell growth and metastasis in bladder cancer (14). In the present study, YRDC-mediated PPI networks in NSCLC were constructed, and a bioinformatics analysis of YRDC was performed using a co-expression analysis. The results revealed that YRDC was involved in regulating spliceosomes, ribosomes, the p53 signaling pathway, proteasomes, the cell cycle and DNA replication.

The most widely used biomarkers in lung cancer currently include cancer antigen (CA) 125 (35), carcinoembryonic antigen and CA153 (36); however, the accuracy of these biomarkers remains limited. A number of novel biomarkers have been identified in NSCLC. For example, B7-H3

expression was upregulated in serum samples and served as a biomarker for the prognosis of NSCLC (37), and mutations in p53 could predict poor prognosis in NSCLC (38,39). Notably, previous studies demonstrated the great prognostic potential of long non-coding (lnc) RNAs in NSCLC (40-42). Downregulation of lncRNA low expression in tumor (40), promoter of CDKN1A antisense DNA damage activated RNA (41) and cancer susceptibility 2 (42) predicts poor prognosis in NSCLC. In the present study, it was observed that YRDC was upregulated in NSCLC samples, and higher expression of YRDC was associated with shorter OS and DFS time in NSCLC. These results suggested that YRDC could serve as a novel biomarker for NSCLC.

There were, however, a number of limitations in the present study. The present study lacks investigations into the molecular mechanisms underlying YRDC-associated regulation of NSCLC progression, and these require further investigation. Of note, the bioinformatics analysis in the present study revealed that YRDC was involved in regulating multiple biological processes. Further validation of the effects of YRDC on these biological processes is required.

In conclusion, to the best of our knowledge, the present study demonstrated for the first time that YRDC was upregulated in and associated with shorter OS and DFS time in NSCLC. Furthermore, knockdown of YRDC suppressed NSCLC cell growth and induced apoptosis *in vitro*. The results from the present study provide evidence to support YRDC as a potential new biomarker for the therapy and prognosis prediction of NSCLC.

Acknowledgements

Not applicable.

Funding

The present study was supported by Effect of miR-30s on the tumor microenvironment of non-small cell lung cance (grant no. 2016HMKY05).

Availability of data and materials

The datasets analyzed in the present study are available in The Cancer Genome Atlas repository, (https://cancergenome.nih.gov/).

Authors' contributions

HS and GZ conceived and designed the experiments, and wrote the article. HS, EZ, ZY, MY and XX performed the experiments. HS, YZ, JN and RL analyzed the data. All authors read and approved the final manuscript.

Ethics approval and consent to participate

Not applicable.

Patient consent for publication

Not applicable.

Competing interests

The authors declare that they have no competing interests.

References

1. Qiao WL, Shi BW, Han YD, Tang HM, Lin J, Hu HY and Lin Q: Testes-specific protease 50 as an independent risk factor for poor prognosis in patients with non-small cell lung cancer. Oncol Lett 15: 8796-8804, 2018.
2. Su Q, Sun YP, Liu YH, Li Z, Yang HY, Sun ZG, Cao BW and Jia JH: Prognostic factors in older patients with advanced non-small cell lung cancer in China. Tumori 100: 69-74, 2014.
3. Shen S, Zhang R, Guo Y, Loehrer E, Wei Y, Zhu Y, Yuan Q, Moran S, Fleischer T, Bjaanaes MM, *et al*: A multi-omic study reveals BTG2 as a reliable prognostic marker for early-stage non-small cell lung cancer. Mol Oncol 12: 913-924, 2018.
4. Zheng X, Cheng M, Fu B, Fan X, Wang Q, Yu X, Sun R, Tian Z and Wei H: Targeting LUNX inhibits non-small cell lung cancer growth and metastasis. Cancer Res 75: 1080-1090, 2015.
5. McCarroll JA, Gan PP, Erlich RB, Liu M, Dwarte T, Sagnella SS, Akerfeldt MC, Yang L, Parker AL, Chang MH, *et al*: TUBB3/βIII-tubulin acts through the PTEN/AKT signaling axis to promote tumorigenesis and anoikis resistance in non-small cell lung cancer. Cancer Res 75: 415-425, 2015.
6. Yue Y, Liu J and He C: RNA N6-methyladenosine methylation in post-transcriptional gene expression regulation. Genes Dev 29: 1343-1355, 2015.
7. Kang BI, Miyauchi K, Matuszewski M, D'Almeida GS, Rubio MAT, Alfonzo JD, Inoue K, Sakaguchi Y, Suzuki T, Sochacka E and Suzuki T: Identification of 2-methylthio cyclic N6-threonylcarbamoyladenosine (ms2ct6A) as a novel RNA modification at position 37 of tRNAs. Nucleic Acids Res 45: 2124-2136, 2017.
8. Vaidyanathan PP, AlSadhan I, Merriman DK, Al-Hashimi HM and Herschlag D: Pseudouridine and N^6-methyladenosine modifications weaken PUF protein/RNA interactions. RNA 23: 611-618, 2017.
9. Zhao BS and He C: Pseudouridine in a new era of RNA modifications. Cell Res 25: 153-154, 2015.
10. Wang CY, Lin MH and Su HT: A method for measuring RNA N 6-methyladenosine modifications in cells and tissues. J Vis Exp 5, 2016.
11. Yu J, Chen M, Huang H, Zhu J, Song H, Zhu J, Park J and Ji SJ: Dynamic m6A modification regulates local translation of mRNA in axons. Nucleic Acids Res 46: 1412-1423, 2018.
12. Thiaville PC, El Yacoubi B, Köhrer C, Thiaville JJ, Deutsch C, Iwata-Reuyl D, Bacusmo JM, Armengaud J, Bessho Y, Wetzel C, *et al*: Essentiality of threonylcarbamoyladenosine (t(6)A), a universal tRNA modification, in bacteria. Mol Microbiol 98: 1199-1221, 2015.
13. El Yacoubi B, Lyons B, Cruz Y, Reddy R, Nordin B, Agnelli F, Williamson JR, Schimmel P, Swairjo MA and de Crécy-Lagard V: The universal YrdC/Sua5 family is required for the formation of threonylcarbamoyladenosine in tRNA. Nucleic Acids Res 37: 2894-2909, 2009.
14. Huang B, Zhai W, Hu G, Huang C, Xie T, Zhang J and Xu Y: MicroRNA-206 acts as a tumor suppressor in bladder cancer via targeting YRDC. Am J Transl Res 8: 4705-4715, 2016.
15. Cui F, Hu J, Ning S, Tan J and Tang H: Overexpression of MCM10 promotes cell proliferation and predicts poor prognosis in prostate cancer. Prostate 78: 1299-1310, 2018.
16. Kroiss A, Vincent S, Decaussin-Petrucci M, Meugnier E, Viallet J, Ruffion A, Chalmel F, Samarut J and Allioli N: Androgen-regulated microRNA-135a decreases prostate cancer cell migration and invasion through downregulating ROCK1 and ROCK2. Oncogene 34: 2846-2855, 2015.
17. Nagy Á, Lánczky A, Menyhárt O and Győrffy B: Validation of miRNA prognostic power in hepatocellular carcinoma using expression data of independent datasets. Sci Rep 8: 9227, 2018.
18. Livak KJ and Schmittgen TD: Analysis of relative gene expression data using real-time quantitative PCR and the 2(-Delta Delta C(T)) method. Methods 25: 402-408, 2001.
19. Zhu T, An S, Choy MT, Zhou J, Wu S, Liu S, Liu B, Yao Z, Zhu X, Wu J and He Z: LncRNA DUXAP9-206 directly binds with Cbl-b to augment EGFR signaling and promotes non-small cell lung cancer progression. J Cell Mol Med 23: 1852-1864, 2019.

20. Sanchez-Palencia A, Gomez-Morales M, Gomez-Capilla JA, Pedraza V, Boyero L, Rosell R and Fárez-Vidal ME: Gene expression profiling reveals novel biomarkers in nonsmall cell lung cancer. Int J Cancer 129: 355-364, 2011.
21. Lu TP, Tsai MH, Lee JM, Hsu CP, Chen PC, Lin CW, Shih JY, Yang PC, Hsiao CK, Lai LC and Chuang EY: Identification of a novel biomarker, SEMA5A, for non-small cell lung carcinoma in nonsmoking women. Cancer Epidemiol Biomarkers Prev 19: 2590-2597, 2010.
22. Hou J, Aerts J, den Hamer B, van Ijcken W, den Bakker M, Riegman P, van der Leest C, van der Spek P, Foekens JA, Hoogsteden HC, *et al*: Gene expression-based classification of non-small cell lung carcinomas and survival prediction. PLoS One 5: e10312, 2010.
23. Szklarczyk D, Franceschini A, Wyder S, Forslund K, Heller D, Huerta-Cepas J, Simonovic M, Roth A, Santos A, Tsafou KP, *et al*: STRING v10: Protein-protein interaction networks, integrated over the tree of life. Nucleic Acids Res 43 (Database Issue): D447-D452, 2015.
24. Shannon P, Markiel A, Ozier O, Baliga NS, Wang JT, Ramage D, Amin N, Schwikowski B and Ideker T: Cytoscape: A software environment for integrated models of biomolecular interaction networks. Genome Res 13: 2498-2504, 2003.
25. Bader GD and Hogue CW: An automated method for finding molecular complexes in large protein interaction networks. BMC Bioinformatics 4: 2, 2003.
26. Bindea G, Mlecnik B, Hackl H, Charoentong P, Tosolini M, Kirilovsky A, Fridman WH, Pagès F, Trajanoski Z and Galon J: ClueGO: A Cytoscape plug-in to decipher functionally grouped gene ontology and pathway annotation networks. Bioinformatics 25: 1091-1093, 2009.
27. Viktorsson K and Lewensohn R: Apoptotic signaling pathways in lung cancer. J Thorac Oncol 2: 175-179, 2007.
28. Liao M: Some features of lung cancer in China. Lung Cancer 10: 107-116, 1993.
29. Xie Y, Zhang Y, Du L, Jiang X, Yan S, Duan W, Li J, Zhan Y, Wang L, Zhang S, *et al*: Circulating long noncoding RNA act as potential novel biomarkers for diagnosis and prognosis of non-small cell lung cancer. Mol Oncol 12: 648-658, 2018.
30. Serresi M, Gargiulo G, Proost N, Siteur B, Cesaroni M, Koppens M, Xie H, Sutherland KD, Hulsman D, Citterio E, *et al*: Polycomb repressive complex 2 is a barrier to KRAS-Driven inflammation and epithelial-mesenchymal transition in non-small-cell lung cancer. Cancer Cell 29: 17-31, 2016.
31. Ludlow AT, Wong MS, Robin JD, Batten K, Yuan L, Lai TP, Dahlson N, Zhang L, Mender I, Tedone E, *et al*: NOVA1 regulates hTERT splicing and cell growth in non-small cell lung cancer. Nat Commun 9: 3112, 2018.
32. Kaczanowska M and Rydén-Aulin M: The YrdC protein-a putative ribosome maturation factor. Biochim Biophys Acta 1727: 87-96, 2005.
33. Lemiere S, Azar R, Belloc F, Gürsel D, Pyronnet S, Bikfalvi A and Auguste P: Overexpression of high molecular weight FGF-2 forms inhibits glioma growth by acting on cell-cycle progression and protein translation. Exp Cell Res 314: 3701-3711, 2008.
34. Brewer JW, Hendershot LM, Sherr CJ and Diehl JA: Mammalian unfolded protein response inhibits cyclin D1 translation and cell-cycle progression. Proc Natl Acad Sci USA 96: 8505-8510, 1999.
35. Nakamura H and Nishimura T: History, molecular features, and clinical importance of conventional serum biomarkers in lung cancer. Surg Today 47: 1037-1059, 2017.
36. Lin Q, Chen XY, Liu WF, Zhu PW, Shi WQ, Li B, Yuan Q, Min YL, Liu JM and Shao Y: Diagnostic value of CA-153 and CYFRA 21-1 in predicting intraocular metastasis in patients with metastatic lung cancer. Cancer Med, Jun 20, 2019 (Epub ahead of print).
37. Zhang G, Xu Y, Lu X, Huang H, Zhou Y, Lu B and Zhang X: Diagnosis value of serum B7-H3 expression in non-small cell lung cancer. Lung Cancer 66: 245-249, 2009.
38. Yu Y, Yang A, Hu S, Zhang J and Yan H: Significance of human papillomavirus 16/18 infection in association with p53 mutation in lung carcinomas. Clin Respir J 7: 27-33, 2013.
39. Niklinska W, Burzykowski T, Chyczewski L and Niklinski J: Expression of vascular endothelial growth factor (VEGF) in non-small cell lung cancer (NSCLC): Association with p53 gene mutation and prognosis. Lung Cancer 34 (Suppl 2): S59-S64, 2001.
40. Li S, Zhao H, Li J, Zhang A and Wang H: Downregulation of long non-coding RNA LET predicts poor prognosis and increases Notch signaling in non-small cell lung cancer. Oncotarget 9: 1156-1168, 2017.
41. Han L, Zhang EB, Yin DD, Kong R, Xu TP, Chen WM, Xia R, Shu YQ and De W: Low expression of long noncoding RNA PANDAR predicts a poor prognosis of non-small cell lung cancer and affects cell apoptosis by regulating Bcl-2. Cell Death Dis 6: e1665, 2015.
42. He X, Liu Z, Su J, Yang J, Yin D, Han L, De W and Guo R: Low expression of long noncoding RNA CASC2 indicates a poor prognosis and regulates cell proliferation in non-small cell lung cancer. Tumour Biol 37: 9503-9510, 2016.